

Cite this: *Phys. Chem. Chem. Phys.*, 2012, **14**, 8859–8865

www.rsc.org/pccp

Effect of hydrogen-bonding on the excited-state reactivity of fullerene derivatives and its impact on the control of the emission polarisation from photopolic single crystals

Guillaume Raffy, Debidas Ray, Cheng-Che Chu, André Del Guerzo* and Dario M. Bassani*

Received 17th February 2012, Accepted 16th April 2012

DOI: 10.1039/c2cp40504k

The kinetics of the irreversible photoinduced switch in polarisation (p) observed in single crystals of a fullerene derivative possessing hydrogen-bonding barbiturate units were investigated using confocal fluorescence microscopy. In the samples investigated, it was found that the maximum luminescence polarisation ($p = 0.78$) is obtained for an orientation of *ca.* 60° from the long axis of the crystal. Upon irradiation at 385 nm, the maximum luminescence polarisation undergoes a rotation of *ca.* 70° with respect to the initial orientation and reaches a new value of $p = 0.40$. The results indicate that the process is not dependent on the orientation of the incident polarised excitation beam and that it is not accompanied by a noticeable change in the photophysical properties of the crystal. Based on these observations, a mechanism is proposed in which photoinduced dimerisation occurs from the lowest energy emissive excimer-like state that acts as a sink for the excitation energy.

Introduction

There are many physical and photophysical properties that can be modified using external stimuli on which are based numerous applications, *e.g.*, sensors, memories, and switches. In particular, the use of light for inscribing information has allowed the emergence of a variety of photolithographic techniques that rely on variations of the physical or optical properties of a material upon irradiation. In all-optical data treatment, light is used to alter a material's response to electronic excitation which results in alteration of its emission (photoluminescence) or absorption (photochromism) spectrum. Materials whose emission polarisation can be switched using light (photopolic materials) are interesting in chiroptical devices and we have recently reported such a material based on a crystalline fullerene solid in which hydrogen-bonding (H-B) interactions are used to guide the formation of linear double-cable fullerene architectures (Fig. 1).¹ Our previous work demonstrated the ability of H-B interactions, generally considered weak intermolecular forces, to control the reaction pathway of excited states.² In the material discussed herein, the H-B units are composed of a barbituric acid moiety that is directly appended to a fullerene core and which presents six H-B donor–acceptor sites which direct the self-assembly of the fullerene units.³ The material exhibits highly polarised photoluminescence originating

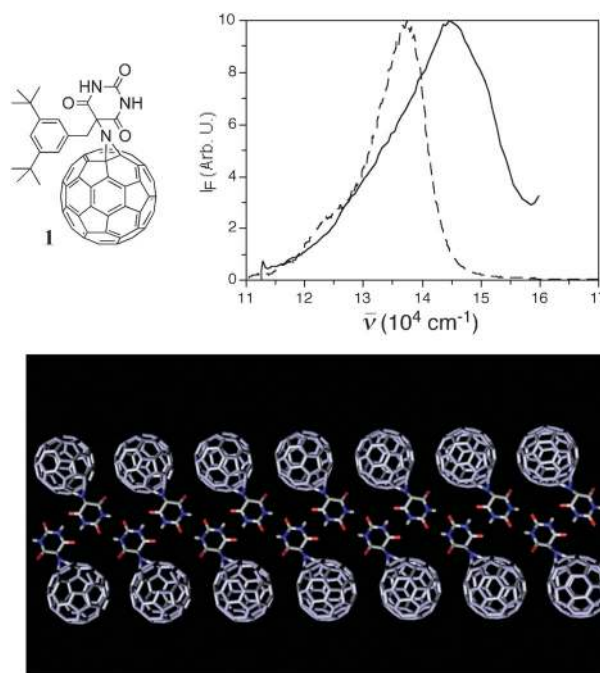


Fig. 1 Chemical structure of compound **1** and its luminescence from 1,2-dichlorobenzene solution ($\lambda_{\text{ex}} = 365$ nm, solid line) and from a single crystal ($\lambda_{\text{ex}} = 385$ nm). Bottom: portion of the solid-state crystal structure of **1** highlighting the H-B ribbon assembly (di-*tert*-butylbenzene groups and solvent omitted for clarity).^{3a}

Univ. Bordeaux, CNRS, ISM UMR 5255 351, Cours de la Libération, 33400 Talence, France. E-mail: d.bassani@ism.u-bordeaux1.fr, a.del-guerzo.ism.u-bordeaux1.fr; Fax: +33 5-4000-6158

from fullerene excimer-like emitting states in which the electronic excitation is delocalized over two or more fullerenes. In one of the more common allotropes, barbituric acid derivatives are known to crystallize into linear H-B ribbons in which each unit is bound to two others *via* the formation of four H-B (Fig. 1).⁴ The distance separating any two barbiturate molecules on each of the two strands composing the ribbon is 12 Å, which is commensurate with the diameter of a fullerene cage (1.1 nm). It was thus anticipated that the linear ribbon structure typical of barbituric acid derivatives could accommodate the presence of a pendant fullerene, as it was indeed observed in the crystal packing arrangement of **1** (Fig. 1).^{3a}

The emission of polarised light from crystalline samples of **1** is attributed to the presence of intermolecular H-B interactions, as neither crystals of pristine fullerene obtained by vacuum-sublimation or from solution-crystallisation show polarised emission.^{3a} Furthermore, it was found that the orientation of the linearly polarised emission could be irreversibly altered by irradiation with 385 nm light.¹ Interestingly, the switch in polarisation is not accompanied by a change of the emission spectrum, which retains the characteristic bathochromic shift attributed to excimer-like emission (Fig. 1). Likewise, irradiation of the sample does not cause any significant variation in the lifetime or in the intensity of the luminescence. Herein, we report a detailed kinetic investigation of the luminescence emission from **1** as a function of irradiation time and sample orientation and show that, within experimental error, the rate of the change in polarisation is independent of the polarisation of the excitation source, and that the amplitude and final orientation only depend on the macroscopic orientation of the sample. From this, a model for the switch in polarisation is proposed, based on the intermolecular photodimerisation of proximal fullerenes along preferential reaction coordinates dictated by the H-B network.

Experimental

Sample preparation: single crystals of **1** were grown by the slow diffusion of chloroform into an *o*-dichlorobenzene solution of **1** and belong to the triclinic space group with cell parameters: C₇₉H₂₅N₃O₃·CHCl₃, mw = 1183.4, *a* = 9.952(2) Å, *b* = 15.876(3) Å, *c* = 15.877(3) Å, α = 77.41(3)°, β = 83.69(3)°, γ = 88.42(3)°, *V* = 2433(8) Å³, *Z* = 2 and ρ_{calc} = 1.615 g cm⁻³. The solution containing the crystals was diluted 20-fold with diethylether, drop cast onto a microscope cover glass, and allowed to dry under ambient conditions.

Microscopy: measurements were performed on a Picoquant Microtime 200 inverted confocal microscope, using a PicoHarp 300 multi-channel single photon counter and two MPD SPAD's. The excitation originates from a frequency doubled Ti-Sa laser (Coherent) tuned at 385 nm with picosecond pulses (4–6 ps) at 4.76 MHz repetition rate. The laser beam is coupled in a polarisation maintaining single mode optical fibre, collimated and finally injected by 90° reflection on a 80%T/20%R spectrally flat beam splitter into the microscope oil immersion objective (100× UPLSAPO, N.A. 1.4). The control of excitation light polarisation was obtained using a Babinet Soleil compensator. The emission is collected by transmission through the same beam splitter and a 470 nm long-pass interferential

filter before being focused on a 50 μm pinhole. Parallel and perpendicular components of the emitted light are split using a polarising beam splitter and two Glan-Thompson polarisers. The instrumental *G*-factor is measured for the emission spectrum of **1** itself, by choosing a reference crystal and taking successively two acquisitions between which both the excitation linear polarisation and the sample have been rotated by 90°. The *G*-factor is then given by the relation $G = ((I_V/I_H)_{0^\circ} \cdot (I_V/I_H)_{90^\circ})^{1/2}$, where *I*_H and *I*_V are the intensities of the horizontal and vertical components of the fluorescence emission, respectively. Total fluorescence intensity was determined according to $I_{\text{tot}} = I_{\parallel} + 2GI_{\perp}$. For emission micro-spectroscopy measurements, after the pinhole, light is diverted into an Andor SR300i spectrometer equipped with a Newton EMCCD.

Results

The samples used for confocal fluorescence measurements were composed of small, isolated triclinic single crystals located with the largest surface co-planar to the microscope slide. Fig. 2 shows a typical area containing several such crystals as observed by optical transmission microscopy. For each crystal, an edge (typically the longest one) was arbitrarily chosen as reference with 0° being defined as parallel to the polarisation of the excitation beam. The polarisation (*p*) of the emission and its dependence with respect to the crystal orientation *p*(θ) can be quantified according to eqn (1) and (2):

$$p = \frac{I_{\parallel} - I_{\perp}}{I_{\parallel} + I_{\perp}} \quad (1)$$

$$p(\theta) = a \sin(\omega(\theta + \varphi)) + c \quad (2)$$

where *I*_∥ and *I*_⊥ are the fluorescence emission intensity components oriented parallel and perpendicular to the polarisation of the excitation beam, respectively, corrected for instrumental response but not for the depolarisation effects of the large numerical aperture objective.⁵ Eqn (2) represents an approximation of a single dipole oscillator model in which *a*, *c*, ω and φ are the maximum amplitude, offset, period and phase of the polarisation with respect to the macroscopic orientation of the crystal.⁶ In the case of **1**, the maximum observed value of *p* (0.78) is very large, clearly indicating that the emission is highly oriented along a specific direction of the molecular crystal.^{3a} In the samples investigated, it was found that the maximum luminescence polarisation was obtained for an orientation of *ca.* 60° from the long axis of the crystal (Fig. 2). To determine the value of *p*, a histogram is built from the values of *I*_∥ and *I*_⊥ collected over time, and the centroid of the Gaussian-like distribution of values is taken as *p* (see Fig. 2 for an example of such a distribution). Incertitude in the determination of *p* arises from errors in ascertaining the absolute crystal orientation with respect to the polarisation of the excitation beam ($\pm 2^\circ$), and from the determination of the value of *p* itself. The precision of the latter is directly linked to the number of counts collected, with more counts giving a narrower distribution but requiring longer irradiation times, which may lead to a change in *p* during data collection when several measurements are taken over the same area. For typical data collection avoiding bleaching or variations in *p* over time, the standard deviation of *p* was determined to be 0.055.

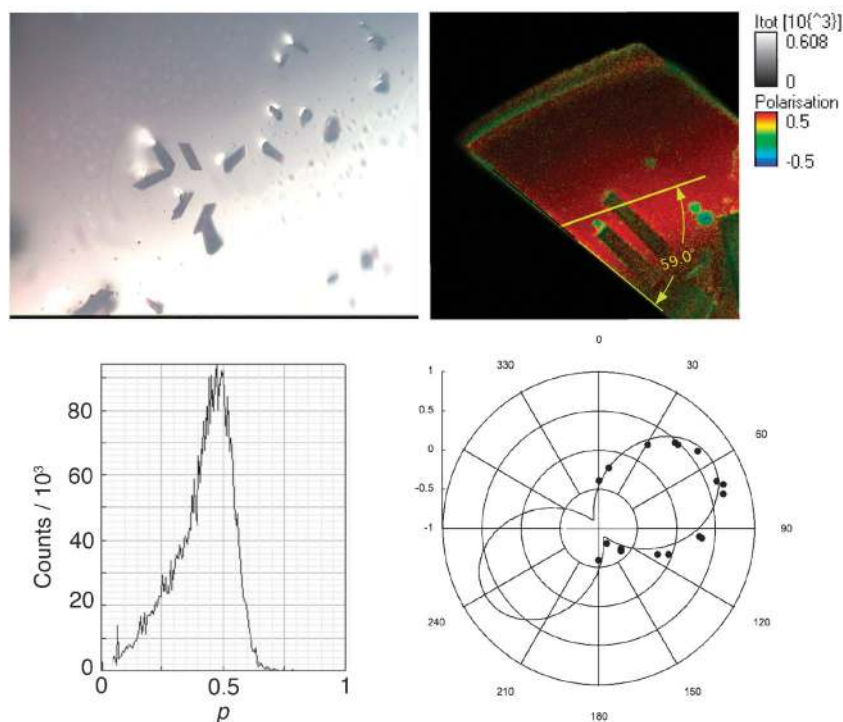


Fig. 2 Optical microscopy image of triclinic crystals of **1** (top left, individual crystals are *ca.* $100\ \mu\text{m} \times 40\ \mu\text{m}$) and confocal fluorescence image (top right, colour represents polarisation, excitation beam is horizontally polarised) of a portion of a triclinic single crystal showing orientation of maximum polarisation (yellow line) determined according to the polar graph below. Bottom left: example of a histogram showing the value of p vs. counts for a given crystal orientation (43°) and the corresponding polar plot of p vs. crystal orientation (bottom right).

Occasionally, needle-shaped crystals could be observed alongside the platelets shown in Fig. 2. These polymorphs also possess strongly polarised emission, as shown in Fig. 3. In this particular example, two areas of the crystal are clearly visible based on the different orientation of the transition dipole moment of the emission and indicate a twinned crystal. Rotation of the sample yields the corresponding polar plots for each area, which indicate that the two emission vectors are oriented with an angle of -16° and $+24^\circ$ with respect to the long edge of the crystal.

Upon irradiation at 385 nm, the emission from crystals of **1** undergoes a change in phase, which depends on the excitation intensity and duration. As stated in the Introduction, the emission collected from the irradiated areas is unaltered with respect to its lifetime, intensity, and wavelength distribution,

but possesses a value of φ which is rotated by $60\text{--}70^\circ$ with respect to the original orientation. Also, the maximum amplitude (a) of the polarisation is reduced from 0.78 to *ca.* 0.42. During our measurements, we noted that thinner crystals ($\sim 1\ \mu\text{m}$) are more photoresponsive than thicker ones, but are more prone to bleaching. The variations in I_{\parallel} and I_{\perp} for a sample that showed negligible bleaching are shown in Fig. 4 along with the best fit to a mono-exponential equation.

To obtain kinetic and angle-dependence information on the photoreaction, we irradiated the sample rotated at different angles relative to a fixed excitation beam polarisation. This approach allows a good control of the purity of the polarisation of the excitation beam. For each measurement, a line was irradiated by scanning the excitation beam over the selected area 200 times. During each writing cycle, each point in the

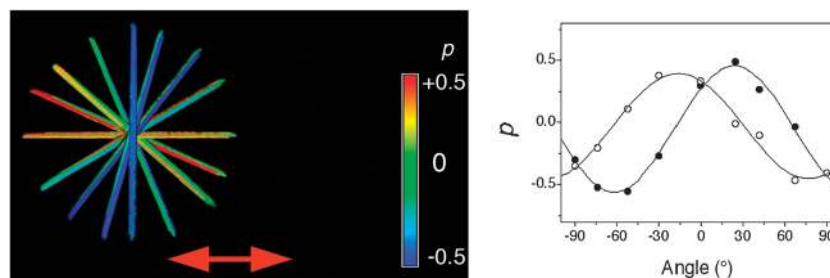


Fig. 3 Polarised emission from a needle-shaped crystal of **1**. Image on the left is an overlay of the emission polarisation (p) for different crystal orientations with respect to the polarisation of the excitation beam (red double arrow) defined as 0° . The values of p for the top half of the crystal (empty circles) and the bottom half of the crystal (filled circles) along with the best fit according to eqn (2) are given on the right. Crystal areas (top and bottom) are defined with the long axis of the crystal at 0° .

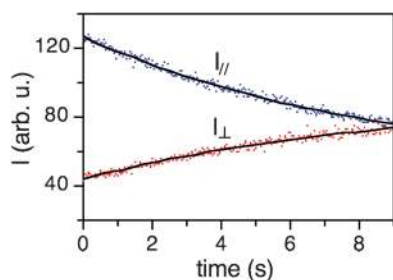


Fig. 4 Variation in I_{\parallel} and I_{\perp} vs. irradiation time for a sample showing negligible bleaching. Solid lines are best fit according to $I = Ae^{-kt}$ with $k = 0.120$ and 0.116 s^{-1} for I_{\parallel} and I_{\perp} , respectively.

line is irradiated for 6 ms, for a total of 1.2 s per line at an incident laser power of $1.4 \mu\text{W}$ (4.4 kW cm^{-2}), with points separated by a distance of 100 nm. Throughout the excitation of the sample, the luminescence emitted is recorded to afford a two-dimensional plot of the emission intensity in each channel (I_{\parallel} and I_{\perp}) as a function of irradiation time. An example of this is shown in Fig. 5 where, for selected orientations, the average value of p vs. irradiation time is plotted. The best fit parameters for the lines shown in Fig. 5 according to $p = A\exp(-kt)$ are collected in Table 1.

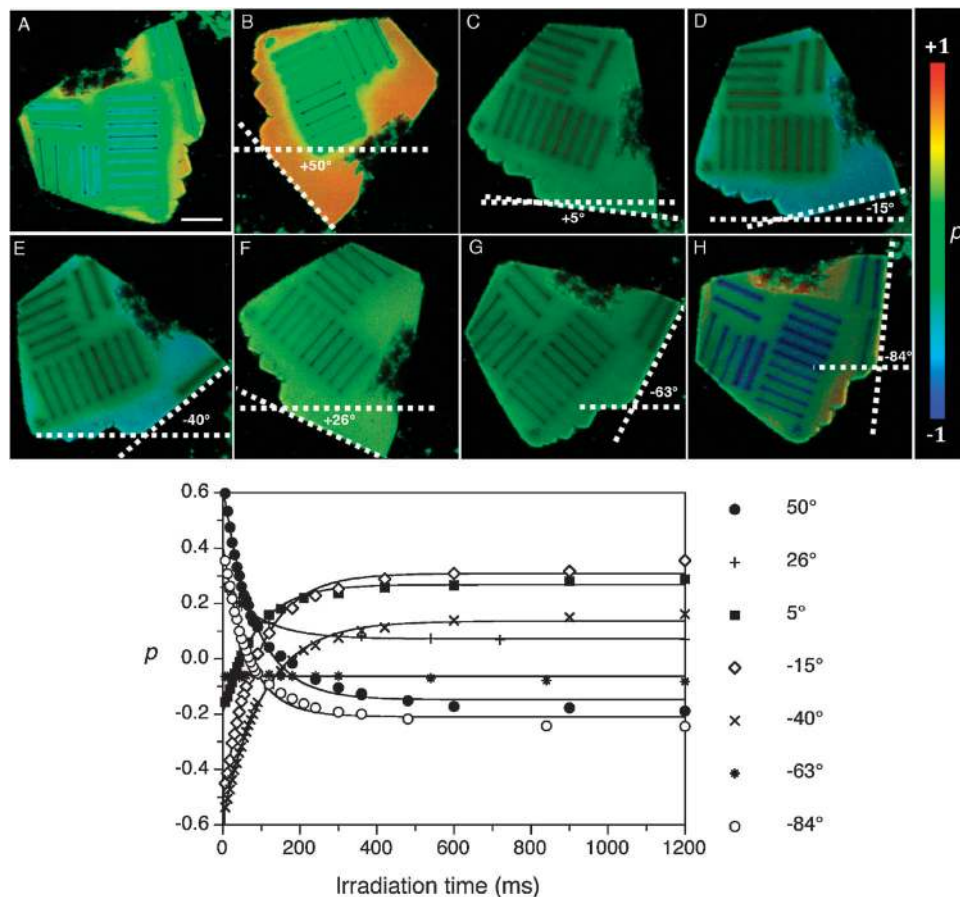


Fig. 5 Confocal fluorescence microscopy images showing polarisation of the emission from a single crystal of **1**. (A) A single crystal of **1** was irradiated along several linear segments, each one for a different orientation of the crystal with respect to the polarisation of the excitation beam (polarised along the horizontal direction). Then, rotation of the crystal (B–H) allows determination of the direction of maximum polarisation of the emission for each line (see the text). For the crystal orientations shown, the polarisation vs. irradiation time is plotted below, along with the best-fit according to a monoexponential function (solid lines represent best fit, see Table 1 for fit parameters).

Discussion

We have previously assigned the emission from single crystals of **1** to be excimer-like, based on the large bathochromic shift observed with respect to solution, analogously to Pippenger *et al.* for single crystals of pristine fullerene.⁷ In this model, absorption of light occurs on a single fullerene chromophore, but the excitation energy is rapidly delocalised over two (or more) fullerenes. In the solid, the reorganisation of the chromophores is limited by the crystal lattice and one may approximate the stabilisation energy of the excited dimer-like state, ΔG_{ex} , to be roughly equal to the difference in the onset of the emission envelope between emission from the locally excited state (observed in solution) and from the excimer-like emitting state. In the case of **1**, this gives a value of $\Delta G_{\text{ex}} \approx -14 \text{ kJ mol}^{-1}$.

In the case of excimer-like emission from single crystals of aromatic chromophores, polarised fluorescence emission is observed when the chromophores are held at a close distance.⁸ Close inspection of the crystal structure of **1** shows that each fullerene moiety is in close contact with four other fullerenes, two of which are located on each side along the molecular hydrogen-bonded ribbon while the other two belong to a proximal in-plane ribbon (Fig. 6). The three pairs of fullerenes

Table 1 Rate constant (k) and amplitude (A) for the irreversible switch in fluorescence polarisation as a function of incident beam irradiation time determined from the analysis of the kinetic information of lines from the sample in Fig. 5 according to $p = A\exp(-k/t)$

Line	Angle/ $^{\circ}$	A	k/s^{-1}	χ^2
1	+50	0.99	11.2	1.1×10^{-2}
2	+26	0.47	10.4	1.2×10^{-4}
3	+5	-0.71	11.8	1.4×10^{-3}
4	-15	-0.91	11.1	4.8×10^{-3}
5	-40	-0.85	9.4	2.6×10^{-3}
6	-84	-0.37	15.2	5.6×10^{-3}

are very similar, but differ in the orientation and distance between fullerenes. Hence, orbital overlap between the fullerenes in each pair will be different. One may therefore expect that, amongst the three possible excimer-like states that may be formed from these pairs of adjacent fullerenes, one would be lower in energy and act as an energy sink for the excitation energy, thus accounting for the initial polarisation of the fluorescence emission. Energy transfer in crystals and organized media (exciton hopping) can be very efficient and occur over long distances.⁹ Unfortunately, we were unable to obtain absolute indexation of the crystal axes, which would allow us to unambiguously assign the direction of the electronic transition dipole moment associated with the polarised emission.¹⁰ However, it is interesting to note that, in their numerous crystallographic analyses of melamine-cyanurate H-B systems that form ribbons akin to those observed for **1**, Whitesides and co-workers found that the direction of the growth of the H-B ribbon is parallel to the longest axis of the crystal.¹¹ A similar situation is also observed in crystals of barbituric acid derivatives, which form long crystals that are also parallel to the H-B ribbon assembly.⁴ This mode of growth is due to a much faster growth of one crystal face with respect to the others, attributed to the occurrence of H-B interactions in the direction of growth of the ribbon. If we assume a similar crystal growth mechanism for **1**, we can observe that the strongest emission is

aligned with an angle of 60° with respect to the longest axis of the crystal (Fig. 2). This would suggest that, assuming that the H-B ribbons grow along the longest axis of the crystal, the excimer-like emission does not originate from fullerenes located within the same H-B ribbon, but from two fullerenes situated in two adjacent H-B ribbons (case B or C in Fig. 6). In B, the two fullerenes are located in close proximity ($d = 3.273 \text{ \AA}$), whereas they are slightly farther apart in C ($d = 3.453 \text{ \AA}$). Differences in the stabilisation energy between these two possible excited-state dimers are thus expected on the basis of the different orbital overlap due to variations in the interchromophore distance and geometry. In support of this, analysis of needle-shaped crystals of **1** (Fig. 3) also reveals that the electronic transition dipole moment is not aligned along the longest axis of the crystal. In Fig. 3, the sample is composed of two areas possessing different values of p , -16° and $+24^{\circ}$, with respect to the polarisation of the excitation beam (crystal parallel to the excitation beam). The fact that the two areas have different orientations of the transition dipole moment, and that both are less than the 60° generally observed for the larger, flat crystals suggests that emission from the sample lies outside the xy plane and that the values measured represent the projection of the electronic transition dipole moment on the plane of the microscope slide.

Upon irradiation ($\lambda_{\text{ex}} = 385 \text{ nm}$), the polarisation of the emission is observed to undergo a change in phase and amplitude (φ and a , respectively, in eqn (2)). The latter is found to decrease from an initial value of *ca.* 0.78 to 0.4, whereas the phase varies by a value of between 65° and 70° . As noted previously, this change in p upon irradiation is not accompanied by a change in the intensity, energy, or lifetime of the emission (which remains monoexponential). The change in p presumably reflects a variation in the orientation of the transition dipole moment of the emission, implying either a rotation of the emitting chromophore or that a new excited state is populated. In view of the rigidity of the crystalline matrix, it is highly unlikely that a fullerene dimer assembly can move, and it seems much more probable that a new

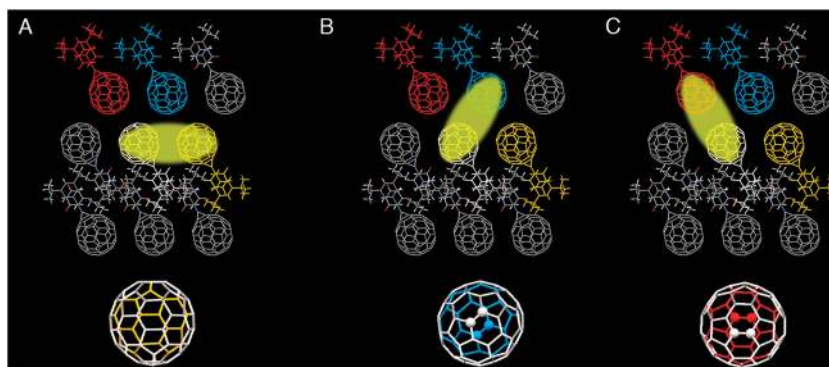


Fig. 6 A cut of the solid-state crystal structure of **1** shows that how each individual fullerene cage is proximal to four other in-plane fullerenes, defining an ensemble of possible excimer-like emitting states in which exciton delocalisation occurs over two nearby fullerene cages. In the case of the fullerene highlighted in white, exciton delocalisation over the nearby fullerene colored in yellow (A) would give rise to an excimer-like state that should not be reactive towards $[2+2]$ dimerisation as none of the reactive 6,6 C=C bonds are in close proximity. In contrast, an excimer-like state formed between the white and the blue fullerenes (B) may undergo photodimerisation since two C=C bonds are in coplanar and in close proximity ($d = 3.273 \text{ \AA}$). An excimer-like state involving the white and the red fullerenes (C) may also undergo photocycloaddition, though the reactive C=C bonds are slightly further apart ($d = 3.453 \text{ \AA}$) than in B. The projection along the $C_{60}-C_{60}$ axis, in which proximal 6,6 C=C bonds are highlighted as spheres, are shown below (no nearby C=C bonds are present in (A)). It is interesting to note that all the possible excimer-like states are rotated by 60° with respect to each other.

excimer-like emitting state – oriented differently from the first – is being populated. The variations in I_{\parallel} and I_{\perp} vs. irradiation time shown in Fig. 4 are described by a pseudo-first order rate equation and confirm that the decrease in one channel is compensated by a commensurate rise in the other channel. This suggests the existence of a first-order photoinduced reaction taking place within the crystal. Reaction with atmospheric oxygen was ruled out on the basis of control experiments under nitrogen vs. ambient environments, which gave similar results. Heating the crystals (110 °C, 30 min) did not induce a recovery of the initial polarisation, indicating that the irreversible switch in polarisation is not due to a small change in geometry within the crystal lattice but to the formation of a thermally stable state. Fullerenes are well-known to undergo photoinduced [2+2] cyclodimerisation across the 6,6 C=C bonds in the solid¹² or in fluid solution when maintained in close proximity using covalent¹³ or supramolecular interactions.^{3b} Based on this, fullerene photodimerisation may be a possible reaction pathway for the excimer-like emitting state. Furthermore, Sun and co-workers showed that the emission from C₁₂₀ photodimers is very similar to that recorded for fullerene C₆₀ and that it does not bear resemblance to the fluorescence emission from the excimer-like emitting states observed in solid samples of fullerenes.¹⁴ This indicates that, despite the close proximity of the fullerene cages, the S₁ energy level of the C₁₂₀ photodimer is higher in energy than the S₁ excimer-like emitting state.

The fullerene pairs from which excimer-like emission is possible are shown in Fig. 6. Although very similar, they differ in distance and mutual orientation of the fullerene cores. To better illustrate the mutual orientation of the nearest 6,6 double bonds between adjacent fullerenes, a horizontal cut between the fullerene pair in which the closest C=C bonds are highlighted as spheres is also presented. In two of these fullerene pairs, the intermolecular distance and orientation of the reactive 6,6 C=C bonds are well suited to undergo cyclodimerisation according to the rules for topochemical transformations set forth by Schmidt and Cohen.¹⁵ In both cases B and C of Fig. 4, 6,6 double bonds that are parallel and in close proximity, separated by a distance of 3.453 Å (in C) and 3.273 Å (in B), are present. For such geometries, the excimer-like emitting states will still generate photoluminescence, but a small fraction may undergo photodimerisation. In the third pair of proximal fullerenes, formed along the axis of the hydrogen-bonded ribbon (case A), the fullerenes are separated by a distance of 3.389 Å but no 6,6 C=C bonds are in close proximity. Photodimerisation from this excimer-like state would thus require a large structural rearrangement, which is disfavoured according to topochemical principles.

From the analysis above, a possible explanation for the observed photopolitic properties of the material emerges: the initially polarised emission is attributed to photoreactive fullerene excimer-like emitting states possessing the lowest energy S₁ state, presumably the one in which the double-bonds are mutually parallel and closest in space (case B). As this is the lowest energy S₁ state, exciton hopping will lead to its efficient population upon excitation of the crystal, and all of the emission collected initially will arise from this excimer-like state. In this model, continued irradiation will eventually lead to dimerisation of these lowest-energy excimer-like emitting states which, according to the work of Sun and co-workers, will no longer exhibit excimer-like

emission as their S₁ ← S₀ transition is similar to that of pristine fullerene. Following photodimerisation of the first lowest-energy excimer-like state, population of the next-lowest lying excited state, located on one of the other two excimer-like emitting states shown in Fig. 6, will become favoured. In all cases, this would lead to a switch in the transition dipole moment of the excimer-like emission that is rotated by 60° from the initial orientation. If an additional excimer that is oriented differently from the first is partially formed upon irradiation, one may expect the combined emission of the two excimers to lead to $\Delta\phi > 60^\circ$. This may explain the slightly larger value of $\Delta\phi = 74^\circ$ measured for the rotation in polarisation that is sometimes observed. The process is illustrated in Fig. 7, in which the excitation is shown to occur on a single fullerene chromophore. If this is indeed the case, we may expect that the rate of change in polarisation is independent of the polarisation of the incident excitation beam as the spherical symmetry of fullerenes excludes polarisation effects. This indeed appears to be the case based on the kinetic analysis shown in Fig. 5. Irrespective of the relative orientation of the polarisation of the excitation beam with respect to the sample, roughly 90% of the complete switch in polarisation is attained within 300 ms. According to eqn (1), and assuming that p is linearly correlated with the population of emitting states that contribute to I_{\parallel} and I_{\perp} , the polarisation should be described by a biexponential function. In practice, however, although clearly not mono-exponential, the experimental data are equally well fit by a single exponential function.¹⁶ The observed decay constants for various crystal orientations collected in Table 1 are quite similar and do not appear to correlate with the polarisation of the excitation beam, indicating that absorption of light is not polarisation-dependent. This would be the case for the excitation of a single fullerene chromophore due to its high symmetry, but not for the excitation of a ground-state fullerene dimer which would be expected to possess electronic transition dipole moments oriented preferentially along the short and long axes of the fullerene pair.⁸

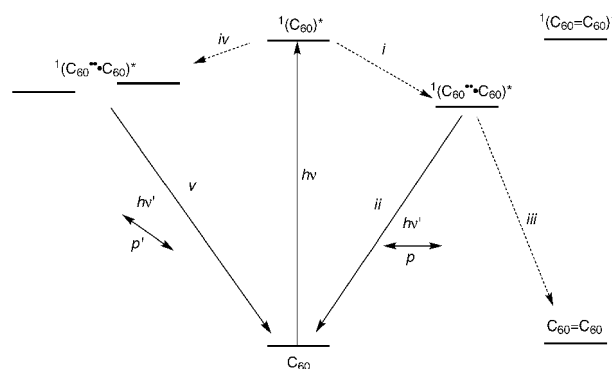


Fig. 7 Proposed reaction scheme to account for the switch in polarisation upon irradiation of single crystals of **1**. Excitation occurs on a single C₆₀ chromophore, which leads to the population of the lowest-energy excimer-like emitting state (C₆₀...C₆₀, process i). The latter can emit with a characteristic polarisation p (ii) or undergo photodimerisation to a C₆₀ photodimer (C₆₀ = C₆₀, process iii). The latter's excited state is higher in energy than other nearby excimer-like emitting states and it is no longer a competitive trap for the excitation energy. Now, other excimer-like states that are oriented differently from the first can become populated through energy transfer (iv) and emit excimer-like emission with a different value of p .

Conclusion

Investigation of the kinetics of the photoinduced switch in polarisation observed in single crystals of **1** has evidenced that the process is not dependent on the orientation of the incident polarised excitation beam. Furthermore, from the relative orientation of the emission with respect to the crystal axes, we deduce that the emission does not arise from excimer-like emitting states originating from fullerenes pertaining to a single H-B ribbon. Based on these observations, and the photoinduced rotation of the emission transition dipole moment, we propose a mechanism in which photoinduced dimerisation of the lowest energy emissive fullerene dimer raises its energy to a level above that of other emissive fullerene dimers, which thus become competitive energy acceptors. These emit light whose transition dipole moment is oriented differently from that of the initially-populated excimer-like emitting state, thus leading to an irreversible switch in emission polarisation. Because both the initial and the final emitting states are nearly identical fullerene excimer-like emitting states, the switch in polarisation is not accompanied by a significant change in emission profile, intensity, or lifetime. Additional effort will be required to positively identify the photoproducts responsible for the switch in polarisation, e.g. using IR or confocal Raman microscopy, though the small sample size and incomplete conversion to the photoproducts make this a very challenging task.

Acknowledgements

Financial support for this work was provided by the Agence Nationale de la Recherche (ANR-08-BLAN-016101), the GIS Aquitaine, and the Région Aquitaine.

References

- G. Raffy, D. Ray, C. C. Chu, A. Del Guerso and D. M. Bassani, *Angew. Chem., Int. Ed.*, 2011, **50**, 9584–9588.
- (a) Y. Molard, D. M. Bassani, J. P. Desvergne, N. Moran and J. H. R. Tucker, *J. Org. Chem.*, 2006, **71**, 8523–8531; (b) Y. Molard, D. M. Bassani, J. P. Desvergne, P. N. Horton, M. B. Hursthouse and J. H. R. Tucker, *Angew. Chem., Int. Ed.*, 2005, **44**, 1072–1075;
- (c) Y. V. Pol, R. Suau, E. Perez-Inestrosa and D. M. Bassani, *Chem. Commun.*, 2004, 1270–1271; (d) V. Darcos, K. Griffith, X. Sallenave, J. P. Desvergne, C. Guyard-Duhayon, B. Hasenknopf and D. M. Bassani, *Photochem. Photobiol. Sci.*, 2003, **2**, 1152–1161; (e) D. M. Bassani, X. Sallenave, V. Darcos and J. P. Desvergne, *Chem. Commun.*, 2001, 1446–1447.
- (a) C. C. Chu, G. Raffy, D. Ray, A. Del Guerso, B. Kauffmann, G. Wantz, L. Hirsch and D. M. Bassani, *J. Am. Chem. Soc.*, 2010, **132**, 12717–12723; (b) N. D. McClenaghan, C. Absalon and D. M. Bassani, *J. Am. Chem. Soc.*, 2003, **125**, 13004–13005.
- B. M. Craven, E. A. Vizzini and M. M. Rodrigues, *Acta Crystallogr., Sect. B: Struct. Crystallogr. Cryst. Chem.*, 1969, **25**, 1978–1993.
- K. Bahlmann and S. W. Hell, *Appl. Phys. Lett.*, 2000, **77**, 621–624.
- S. Inoue, O. Shimomura, M. Goda, M. Shribak and P. T. Tran, *Proc. Natl. Acad. Sci. U. S. A.*, 2002, **99**, 4272–4277.
- P. M. Pippenger, R. D. Averitt, V. O. Papanyan, P. Nordlander and N. J. Halas, *J. Phys. Chem.*, 1996, **100**, 2854–2861.
- J. B. Birks, *Photophysics of Aromatic Molecules*, Wiley, New York, 1970.
- (a) L. Poulsen, M. Jazdzzyk, J. E. Communal, J. C. Sancho-Garcia, A. Mura, G. Bongiovanni, D. Beljonne, J. Cornil, M. Hanack, H. J. Egelhaaf and J. Gierschner, *J. Am. Chem. Soc.*, 2007, **129**, 8585–8593; (b) A. Del Guerso, A. G. L. Olive, J. Reichwagen, H. Hopf and J.-P. Desvergne, *J. Am. Chem. Soc.*, 2005, **127**, 17984; (c) B. A. Gregg, J. Sprague and M. W. Peterson, *J. Phys. Chem. B*, 1997, **101**, 5362–5369.
- The crystal structure was obtained on the Proximal line of the Soleil synchrotron, which was not equipped with a CCD camera.
- (a) G. M. Whitesides, E. E. Simanek, J. P. Mathias, C. T. Seto, D. N. Chin, M. Mammen and D. M. Gordon, *Acc. Chem. Res.*, 1995, **28**, 37–44; (b) J. A. Zerkowski, J. C. Macdonald, C. T. Seto, D. A. Wierda and G. M. Whitesides, *J. Am. Chem. Soc.*, 1994, **116**, 2382–2391; (c) C. T. Seto and G. M. Whitesides, *J. Am. Chem. Soc.*, 1990, **112**, 6409–6411.
- (a) A. M. Rao, P. Zhou, K. A. Wang, G. T. Hager, J. M. Holden, Y. Wang, W. T. Lee, X. X. Bi, P. C. Eklund, D. S. Cornett, M. A. Duncan and I. J. Amster, *Science*, 1993, **259**, 955–957; (b) Y. P. Sun, B. Ma, C. E. Bunker and B. Liu, *J. Am. Chem. Soc.*, 1995, **117**, 12705–12711.
- J. Knol and J. C. Hummelen, *J. Am. Chem. Soc.*, 2000, **122**, 3226–3227.
- B. Ma, J. E. Riggs and Y.-P. Sun, *J. Phys. Chem. B*, 1998, **102**, 5999–6009.
- (a) G. M. J. Schmidt, *J. Chem. Soc.*, 1964, 2014–2021; (b) M. D. Cohen and G. M. J. Schmidt, *J. Chem. Soc.*, 1964, 1996–2000.
- This may be due to the fact that other processes, such as energy transfer and bleaching, are not taken into account.